Enhanced Calvarial Bone Healing in CD11c-TLR4$^{-/-}$ and MyD88$^{-/-}$ Mice

Dan Wang, D.M.D., Ph.D.
Gwen M. Taylor, Ph.D.
James R. Gilbert, Ph.D.
Joseph E. Losee, M.D.
Chhinder P. Sodhi, Ph.D.
David J. Hackam, M.D., Ph.D.
Timothy R. Billiar, M.D.
Gregory M. Cooper, Ph.D.

Shanghai, People's Republic of China; Pittsburgh, Pa.; and Baltimore, Md.

Background: Inflammation is integral to the injury response. The inflammatory response is essential to the host defense against infection and also to tissue regeneration and repair. Toll-like receptors (TLRs) are critical activators of the innate immune response and present attractive therapeutic targets for inflammation-modulated tissue regeneration. The authors' previous study showed that depletion of TLR4 resulted in accelerated skull bone healing concurrent with increased expression of osteoclastogenic genes. As such, in the present study, the authors used various knockout mouse models for TLR4 and its associated signaling mediators as tools to further understand the role of Toll-like receptor–mediated inflammation in calvarial bone healing.

Methods: Calvarial defects (1.8-mm diameter) were created in wild-type, TLR4 knockout (TLR4$^{-/-}$), TLR2$^{-/-}$, MyD88$^{-/-}$, TRIF$^{-/-}$, TLR4 knockout in myeloid cell (Lyz-TLR4$^{-/-}$), and TLR4 knockout in dendritic-lineage cell (CD11c-TLR4$^{-/-}$) mice. Bone healing was examined using micro–computed tomographic, histologic, and histomorphometric analyses.

Results: Micro–computed tomographic and histomorphometric analyses revealed that TLR4-deficient mice (TLR4$^{-/-}$, Lyz-TLR4$^{-/-}$, and CD11c-TLR4$^{-/-}$) exhibited a faster intramembraneous healing response at postoperative day 7, whereas MyD88$^{-/-}$ and CD11c-TLR4$^{-/-}$ mice showed enhanced bone healing at day 28.

Conclusions: The authors' data suggest a detrimental role for TLR4 in CD11c^{+} cells, mediated by Myd88 signaling, during calvarial bone healing. The authors have demonstrated that Toll-like receptor signaling components affect calvarial bone healing, establishing a link between the skeletal and immune systems during craniofacial bone healing. Toll-like receptor signaling components might be used to initiate enhanced healing in bone defects to improve clinical outcomes. (*Plast. Reconstr. Surg.* 139: 933e, 2017.)

Craniofacial skeletal injuries have a tremendous economical, biological, and social impact, with an estimated 592,000 cranial operations performed annually in the United States.[1] Oftentimes, current treatment strategies of craniofacial defects are inadequate. These shortcomings have driven various efforts to develop and improve existing therapies for craniofacial reconstruction.

One developing strategy is to modulate the host inflammatory response to induce tissue regeneration. Clinically, inflammation is often associated

From the Department of Stomatology, Tenth People's Hospital of Tongji University; the Departments of Plastic Surgery, Surgery, Oral Biology, and Bioengineering, University of Pittsburgh; and the Department of Surgery, The Johns Hopkins University.

Received for publication March 1, 2016; accepted October 27, 2016.

Presented in part at the 58th Annual Meeting of the Plastic Surgery Research Council, in Santa Monica, California, May 2 through 4, 2013.

DOI: 10.1097/PRS.0000000000003206

Disclosure: *The authors have no financial interest to declare in relation to the content of this article.*

Supplemental digital content is available for this article. A direct URL citation appears in the text; simply type the URL address into any Web browser to access this content. A clickable link to the material is provided in the HTML text of this article on the *Journal*'s website (www.PRSJournal.com).

with tissue destruction, poor healing potential, surgical-site infection, and negative patient outcomes. However, recent research has sought to harness and modulate the host inflammatory response to facilitate tissue regeneration, including regeneration of cardiac and musculoskeletal tissues.[2] Broadly, the early events in the inflammatory cascade serve to recruit inflammatory and progenitor cells and also promote angiogenesis.[3]

Although the inflammatory response is a complex ensemble of intracellular and extracellular signals, the early cascade can be simplified as leading to two diverging pathways: a regenerative pathway and a destructive pathway. Mounting evidence indicates that these early events determine the nature of healing response dependent on which pathway is initiated.[3–5] As a result, efforts have been made to improve craniofacial skeleton repair either by enhancing the regenerative effects of inflammation or by inhibiting the destructive effects of inflammation. Therefore, detailed understanding of the interplay between the molecular mechanisms of host inflammation and skeletal regeneration may lead to therapies targeted to control and modulate the inflammatory response to augment bone healing.

Toll-like receptors (TLRs) are important mediators of the immune response that recognize a wide range of pathogen-associated molecular patterns and damage-associated molecular patterns in response to infection, injury, stress, and cellular necrosis.[6] In addition to their roles in host defense against microbial infection, Toll-like receptors are also involved in tissue fibrosis, tissue homeostasis, and wound healing in the nervous, digestive, cardiovascular, and musculoskeletal systems, through multiple mechanisms including limiting the extent of initial tissue injury and stimulating the repair cascade.[6] Myeloid differentiation primary response gene 88 (MyD88) and TIR-domain-containing adapter-inducing interferon-β (TRIF) are the two main adaptor proteins of Toll-like receptor signaling that mediate downstream pathways, including nuclear factor kappa B, interferon regulatory factor-1, and mitogen-activated protein kinases.[6] Although most Toll-like receptors signal only through the MyD88 pathway, TLR4 is unique in that it also uses the TRIF pathway.[6]

Distinction has been made in the contribution of MyD88- and TRIF-mediated signaling pathways to TLR4-driven responses to injury. For example, studies have demonstrated that MyD88 signaling contributes to ischemic brain damage[7,8] and hindlimb ischemia,[9] whereas TRIF-mediated signaling exerts a neuroprotective effect against cerebral ischemia.[10] Conversely, MyD88-dependent signaling has protective effects in models of cardiac and pulmonary injury, radiation-induced lung injury, and intestinal ischemia.[11] In short, the functional consequences of Toll-like receptor activation on tissue homeostasis and regeneration are strongly dependent on organ setting, mode of activation, and mode of injury. As such, understanding the mechanistic aspects of Toll-like receptor signal transduction during bone healing will be crucial for appreciating their contributions to tissue regeneration at the cellular level.

Studies have shown an essential involvement of Toll-like receptors in skeletal homeostasis,[12,13] although the specific cellular contribution is unknown. Multiple cell types are involved in injury-stimulated bone regeneration,[14] including inflammatory cells (platelets, macrophages, lymphocytes, and granulocytes) that migrate into the fracture hematoma and regulate inflammation and tissue regeneration.[15] For example, macrophages infiltrate into the wound bed within 48 to 96 hours after injury, participating in the inflammatory response and débridement process by means of phagocytosis activity and reactive radical release. Dendritic cells regulate the highly pathogen-specific adaptive immune responses and are critical in the development of immunologic memory and tolerance.[16] Because there is differential Toll-like receptor expression among different immune cells,[17] understanding how lineage-specific Toll-like receptor inactivation affects injuries and subsequent healing may provide insight into the mechanisms of inflammation during bone regeneration and repair under various clinical settings.

To better understand the cellular and molecular mechanisms by which TLR4 influences calvarial bone healing, we endeavored to assess bone healing after calvarial bone injury in different mouse strains that lacked key mediators of Toll-like receptor signaling (MyD88 or TRIF) or lacked TLR4 expression specifically in myeloid (Lyz^+) or dendritic ($CD11c^+$) cells. The current study was designed to test the hypothesis that TLR4 signaling through TRIF is detrimental to bone healing.

MATERIALS AND METHODS

Mouse Strains and Derivation

Wild-type mice were obtained from The Jackson Laboratory (Bar Harbor, Me.). $TLR4^{-/-}$, $TLR2^{-/-}$, Lyz-$TLR4^{-/-}$, CD11c-$TLR4^{-/-}$, $MyD88^{-/-}$, and $TRIF^{-/-}$ mice mentioned in this study were generated from an ongoing breeding colony at the University of Pittsburgh as

described.[17] Female mice from all strains, between 10 and 12 weeks of age and weighing 20 to 30 g, were used in this study. All mice were maintained in the Rangos Research Center Animal Facility at Children's Hospital of Pittsburgh of the University of Pittsburgh Medical Center with a 12-hour light/dark cycle and free access to standard laboratory food and water. All procedures were carried out in accordance with regulations regarding the care and use of experimental animals published by the National Institutes of Health and was approved by the University of Pittsburgh Institutional Animal Use and Care Committee.

Surgical Procedure

Mice were anesthetized with isoflurane (2% by inhalation) and their scalps were shaved and cleaned with povidone-iodine. Under sterile conditions, a 1.8-mm circular bone defect was created in the skull parietal bone using a trephine with an outer diameter of 1.8 mm as described previously.[18] Ketoprofen, 1 mg/kg (Fort Dodge Animal Health, Fort Dodge, Iowa), was administered as an analgesic immediately and 2 days after surgery. Mice were killed by means of carbon dioxide asphyxiation followed by cervical dislocation on postoperative days 7 and 28.

Live Micro–Computed Tomographic Analyses

Calvarial defect healing was analyzed using a live high-resolution micro–computed tomographic system (Inveon microCT; Siemens, Erlangen, Germany). At postoperative days 7, 14, and 28, bone healing of wild-type, TLR4$^{-/-}$, TLR2$^{-/-}$, Lyz-TLR4$^{-/-}$, CD11c-TLR4$^{-/-}$, MyD88$^{-/-}$, and TRIF$^{-/-}$ mice (average, 10 mice per group) was analyzed using live micro–computed tomography with a fixed isotropic voxel size of 62.4 μm. Three-dimensional images were reconstructed using Amira 5.4 3D software (FEI Visualization Sciences Group, Burlington, Mass.). Quantitative data were analyzed using OsiriX software (Pixmeo, Bernex, Switzerland) with a fixed threshold of −330, and a region of interest of 4.0 mm^2 x 2.09 mm was defined. Standard micro–computed tomographic measurements (regenerated bone volume = bone volume within the region of interest at days 7, 14, and 28 − bone volume at day 0) were calculated for each sample using OsiriX software.

Histology and Histomorphometric Analysis

All mice were killed on postoperative day 28. Wild-type, TLR4$^{-/-}$, Lyz-TLR4$^{-/-}$, and CD11c-TLR4$^{-/-}$ mice were also killed at postoperative day 7. Calvariae and surrounding soft tissues (e.g., skin, brain) were harvested, fixed in 4% neutral buffered paraformaldehyde for 24 hours, decalcified in 10% ethylenediaminetetraacetic acid, and dehydrated through a series of alcohols and embedment in paraffin. Paraffin-embedded specimens were sectioned through the coronal plane at a thickness of 5 to 6 μm. Slides were stained with Harris' hematoxylin and eosin (Surgipath Medical Industries, Richmond, Ill.) for conventional, qualitative bright-field light microscopy. All specimens were examined at 25×, 100×, 200×, and 400× magnifications.

Russell-Movat pentachrome staining (American MasterTech, Lodi, Calif.) was performed to further differentiate the following tissues within the defect: hematoma/fibrin (intense red) and elastic fibers (black), and granulation/fibrous tissue (green or light blue), newly-formed woven bone (yellow), and lamellar bone (red) formation and degradation. All specimens were examined at 25×, 50×, 100×, and 200× magnifications.

Histomorphometric analysis was performed to quantify the two-dimensional area of new bone formation using a Leica MZ12 Stereo Zoom microscope (Leica Microsystems, Buffalo Grove, Ill.) and Northern Eclipse (v5.0) image analysis software (Empix Imaging, Inc., Mississauga, Ontario, Canada). Histomorphometric measurements were determined using three to five slides per animal. New bone area was calculated as the sum of the areas of each bone section, including within the defect and on both the endocortical and ectocortical sides of calvarial bone.

Statistical Analyses

Statistical analyses were performed using IBM SPSS Version 20.0 software (IBM Corp., Armonk, N.Y.). Newly regenerated bone volumes collected from micro–computed tomographic analysis were compared using a group × time point (7 × 3) two-way analysis of variance followed by a group × time point (7 × 1) split-plot one-way analysis of variance and post hoc least significant difference tests to compare each group over time. Mean areas of newly formed bone calculated from histomorphometric measurements were analyzed using one-way analysis of variance and post hoc least significant difference tests for multiple comparisons at each time point. A value of $p \leq 0.05$ was considered significant.

RESULTS

Enhanced Calvarial Bone Healing in CD11C-TLR4$^{-/-}$ and Myd88$^{-/-}$ Mice at Day 28

Mineralized tissue was observed around the defect margins of TLR4$^{-/-}$, Lyz-TLR4$^{-/-}$, and

CD11c-TLR4$^{-/-}$ mice at day 7, suggesting a faster healing response compared with wild-type control (Fig. 1). Improved overall healing of calvarial defects was observed in CD11c-TLR4$^{-/-}$ mice and MyD88$^{-/-}$ mice compared with wild-type control mice at day 28 (Fig. 1). Detailed regenerated bone volume data from micro–computed tomographic measurements of all groups at different time points are shown in Fig. 2, *above*, *left*. The greatest difference in bone healing was observed at day 7 (Fig. 2, *above*, *right*). Differences in healing were less pronounced at day 28 (Fig. 2, *below*, *right*). Two-way analysis of variance of bone volume analyses showed that significant differences were detected within time interactions (days 7, 14, and 28; $p < 0.001$) and within group interactions (all seven experimental groups; $p < 0.001$), whereas no significant difference was detected within group × time interactions. At postoperative day 7, one-way analysis of variance analyses that bone volume measurements were significantly larger in the TLR4$^{-/-}$ (0.141 ± 0.019 mm^3; $p < 0.05$), Lyz-TLR4$^{-/-}$ (0.179 ± 0.029 mm^3; $p < 0.001$), and CD11c-TLR4$^{-/-}$ (0.183 ± 0.021 mm^3; $p < 0.001$) groups than in the wild-type group. At day 14, bone volume measurements were significantly larger in TLR4$^{-/-}$ (0.223 ± 0.035 mm^3; $p < 0.05$), Lyz-TLR4$^{-/-}$ (0.231 ± 0.032 mm^3; $p < 0.05$), CD11c-TLR4$^{-/-}$ (0.254 ± 0.021 mm^3; $p < 0.05$), and MyD88$^{-/-}$ groups (0.227 ± 0.062; $p < 0.05$) compared with the wild-type group. At postoperative day 28, bone volume measurements were significantly larger in CD11c-TLR4$^{-/-}$ (0.43 ± 0.025; $p < 0.05$) and MyD88$^{-/-}$ groups (0.369 ± 0.046; $p < 0.05$) compared with the wild-type group (0.232 ± 0.036 mm^3) (Fig. 2, *above*, *right* and *below*).

Faster Intramembranous Bone Formation in TLR4$^{-/-}$, Lyz-TLR4$^{-/-}$, and CD11C-TLR4$^{-/-}$ Mice

Disorganized connective tissue completely filled the bone defect by day 7. Cellularized newly regenerated woven bone, indicated by positive saffron yellow staining, was observed mainly on the endocortical side of the calvarial bone lateral to the defect perimeter in all groups (Fig. 3, *left*). Typical large, rounded osteoblasts were detected on the surface of the newly formed woven bone of the three knockout mice groups (Fig. 3, *below*, *left*). Pentachrome staining showed larger areas of newly formed bone in TLR4$^{-/-}$, Lyz-TLR4$^{-/-}$, and CD11c-TLR4$^{-/-}$ mice compared with wild-type mice on day 7 (Fig. 3, *left*). One-way analysis of variance showed significantly larger areas of newly regenerated bone area in TLR4$^{-/-}$, Lyz-TLR4$^{-/-}$, and CD11c-TLR4$^{-/-}$ mice compared with wild-type mice on day 7 ($p < 0.05$) (Fig. 3, *below*, *right*). No significant differences in newly regenerated bone areas were observed among TLR4$^{-/-}$, Lyz-TLR4$^{-/-}$, and CD11c-TLR4$^{-/-}$ groups (Fig. 3, *below*, *right*).

All groups showed similar histologic healing patterns, and complete bone healing was not observed on postoperative day 28 (Fig. 4) (hematoxylin and eosin–stained images not shown). Periosteum and soft connective tissue became much thinner, more dense, and better organized on day 28. Regenerated bone was seen along the dural surface of the calvarial bone and along the defect perimeter. Fewer typical rounded osteoblasts were identified on the newly formed bone surface compared to day 7. All groups showed bone remodeling as indicated with acid fuchsin red-positive staining (Fig. 4, *left*). One-way analysis of variance showed no significant differences in the amount of newly regenerated bone areas measured by histomorphometry (Fig. 4, *below*, *right*).

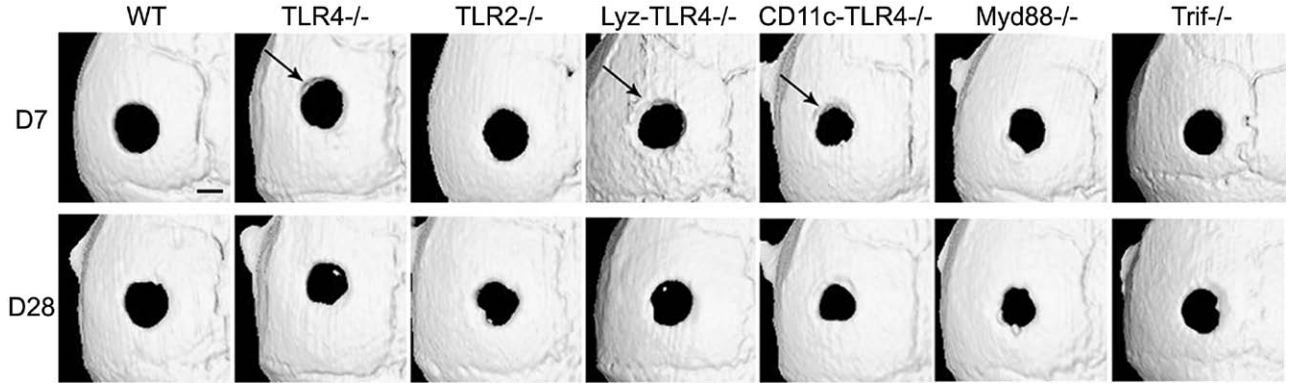

Fig. 1. Live micro–computed tomographic analyses of all mouse groups. Representative three-dimensional reconstructions of calvarial defects in the transverse plane at postoperative days 7 and 28. Faster healing was evident in TLR4$^{-/-}$, Lyz-TLR4$^{-/-}$, and CD11c-TLR4$^{-/-}$ mice as indicated by mineralized tissue around the defect edges on day 7. Smaller defect areas are shown in CD11c-TLR4$^{-/-}$ and MyD88$^{-/-}$ mice compared with wild-type mice on day 28.

Regenerated BV (mm^3)

	D7	D14	D28
WT	0.028+/-0.029	0.086+/-0.05	0.232+/-0.036
TLR4-/-	0.141+/-0.019	0.223+/-0.035	0.295+/-0.038
TLR2-/-	0.045+/-0.041	0.173+/-0.068	0.359+/-0.06
Lyz-/-	0.179+/-0.029	0.231+/-0.032	0.34+/-0.029
CD11c-/-	0.183+/-0.021	0.254+/-0.021	0.43+/-0.025
Myd88-/-	0.115+/-0.062	0.227+/-0.062	0.369+/-0.046
Trif-/-	0.04+/-0.033	0.11+/-0.031	0.357+/-0.048

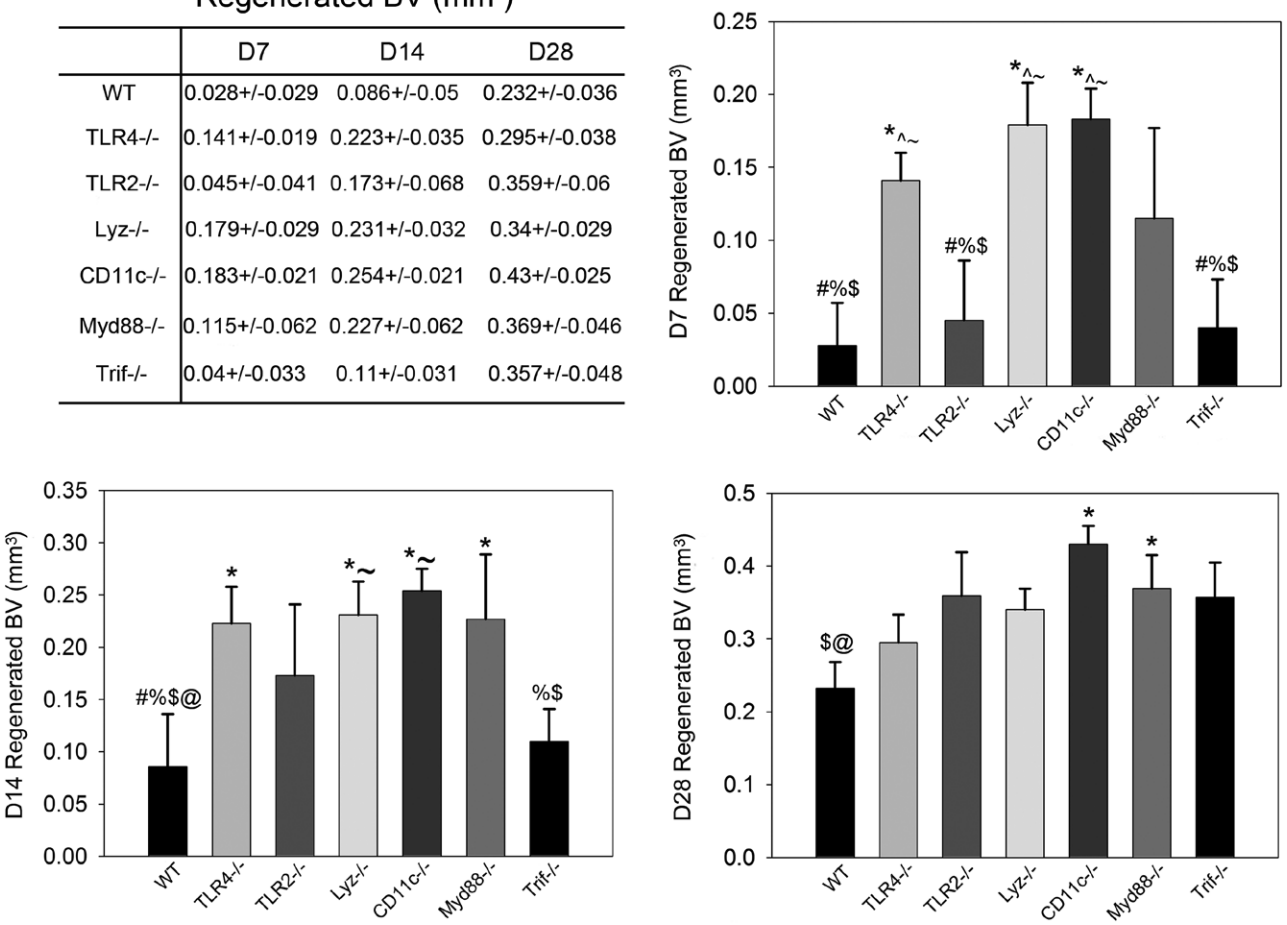

Fig. 2. (*Above*, *left*) Table shows the regenerated bone volume measurements based on micro–computed tomographic analyses at different time points (mean ± SEM). (*Above*, *right* and *below*) Two-way analysis of variance of regenerated bone volume–based micro–computed tomographic measurements showed no significant differences within group (all mouse groups) × time interactions (days 7, 14, and 28). One-way analysis of variance showed that bone volumes were significantly larger in TLR4$^{-/-}$, Lyz-TLR4$^{-/-}$, and CD11c-TLR4$^{-/-}$ groups than in the wild-type group at day 7; in TLR4$^{-/-}$, Lyz-TLR4$^{-/-}$, CD11c-TLR4$^{-/-}$, and MyD88$^{-/-}$ groups than in the wild-type group at day 14; and in CD11c-TLR4$^{-/-}$ and MyD88$^{-/-}$ groups compared with the wild-type group on day 28. More detailed comparisons among groups at different time points are shown in Figure 3. *Scale bar* = 500 μm. *BV*, bone volume within region of interest. *Compared to wild-type; #compared to TLR4$^{-/-}$; ^compared to TLR2$^{-/-}$; %compared to Lyz-TLR4$^{-/-}$; $compared to CD11c-TLR4$^{-/-}$; ~compared to TRIF$^{-/-}$; @compared to MyD88$^{-/-}$ ($p < 0.05$).

DISCUSSION

Toll-like receptors are critical activators of the innate immune response and are attractive therapeutic targets for inflammation-modulated tissue regeneration.[19] The role of inflammation on long bone healing has been extensively investigated; however, its impact within craniofacial settings is not well understood. In this study, we examined the calvarial bone healing in mice lacking important mediators of Toll-like receptor signaling pathways, aiming to understand the role of Toll-like receptor signaling on calvarial defect healing. Remarkably, we found that CD11c^{+} cells expressing TLR4 might be detrimental to bone healing through the MyD88 pathway, suggesting a regulatory role of these Toll-like receptor pathway mediators in calvarial fracture repair.

Studies have suggested important roles of TLR4/MyD88 and TLR2/MyD88 signaling pathways in regulating inflammation and bone metabolism in various osteolytic diseases.[20,21] Despite these identified interactions, the involvement of MyD88 signaling in a noncompromised fracture healing process has not been investigated. In this study, we observed the calvarial bone healing process in TLR2$^{-/-}$, TLR4$^{-/-}$, MyD88$^{-/-}$, and TRIF$^{-/-}$ mice. In the current study, we did not observe differences in bone healing between TLR2$^{-/-}$ and TLR4$^{-/-}$ mice, but did observe enhanced bone healing in MyD88$^{-/-}$ mice compared with wild-type mice at

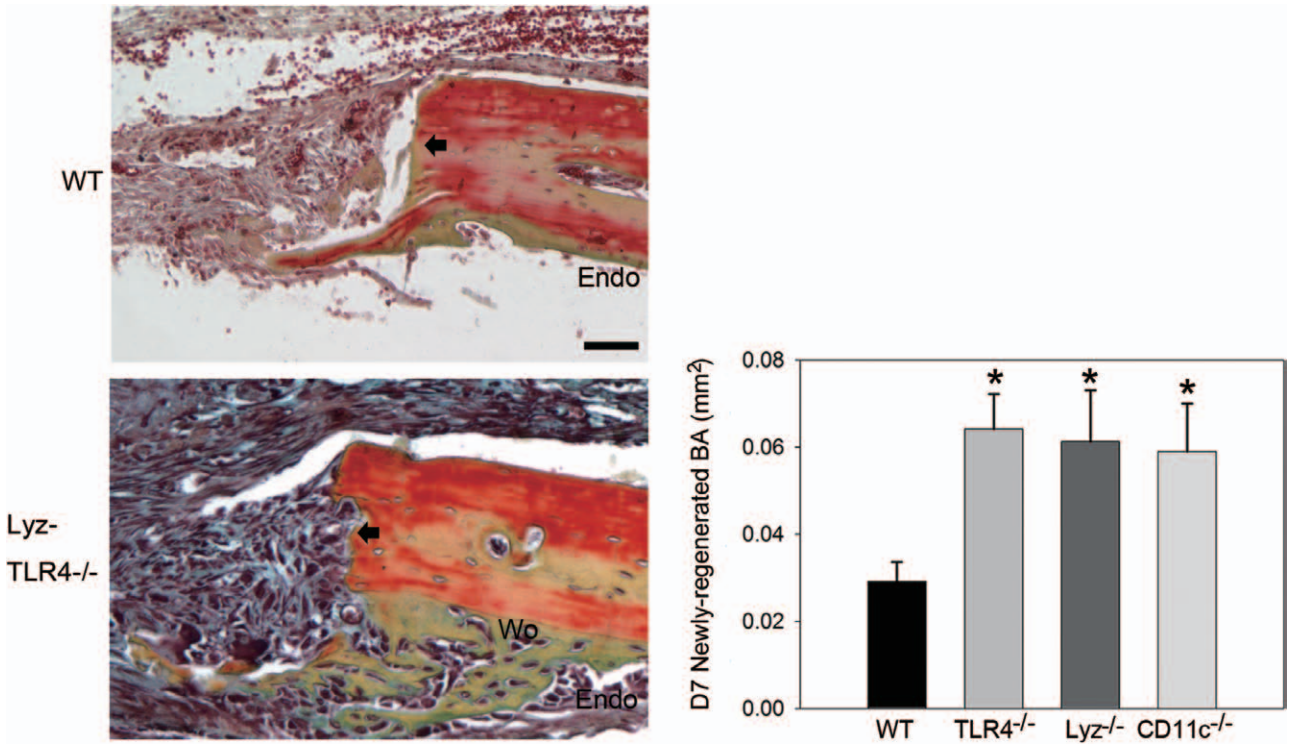

Fig. 3. Histology and histomorphometric analyses of calvarial bone repair at postoperative day 7. (*Left*) Representative pentachrome-stained images of wild-type and Lyz-TLR4$^{-/-}$ mice on day 7. We used pentachrome-stained images of Lyz-TLR4$^{-/-}$ mice to represent TLR4$^{-/-}$ and CD11c-TLR4$^{-/-}$ groups. Larger areas of woven bone, indicated by saffron yellow staining, and more infiltration osteoblasts were observed in TLR4$^{-/-}$, Lyz-TLR4$^{-/-}$, and CD11c-TLR4$^{-/-}$ mice compared with wild-type mice. (*Below*, *right*) Histomorphometric analysis revealed larger areas of newly regenerated bone (*BA*) in the three knockout mice groups compared with the wild-type group. Comparable healing was observed in the three knockout groups on day 7. *Scale bar* = 50 μm. *Arrow*, defect margin; *Endo*, endocortical side; *Wo*, woven bone. *$p < 0.05$ compared to wild-type mice.

day 28. These observations may be attributed to the ability of Toll-like receptors to reciprocally compensate for each other's loss of gene function, as MyD88 is an important adaptor protein for the majority of Toll-like receptor signaling.[22,23] Therefore, it has been observed that loss of MyD88 function has a large impact on downstream Toll-like receptor signaling pathways, the immune response against pathogens, and tissue regeneration after injury.[24] In our study, we showed that MyD88 has a detrimental role in bone regeneration because enhanced bone healing was observed in MyD88$^{-/-}$ mice and not TRIF$^{-/-}$ mice compared to wild-type mice on day 28. The accelerated bone healing phenotype observed within this model does not appear to be mediated through the TRIF-dependent pathway, and may instead be mediated through the MyD88-dependent pathway.

In our previous study,[18] enhanced osteoclastogenesis correlated with accelerated skull healing in TLR4$^{-/-}$ mice. We observed faster bone healing and increased expression of *rankl* in TLR4$^{-/-}$ mice compared with wild-type mice.[18] Because both myeloid and dendritic cells give rise to osteoclasts, we further dissected the role of TLR4 signaling in these cells to understand their role in calvarial bone healing. To specifically knock out TLR4 expression in myeloid cells (Lyz-TLR4$^{-/-}$) and dendritic cells (CD11c-TLR4$^{-/-}$), the Cre-*loxP* technique was used in conjunction with lysozyme (*lyz*) and CD11c (*cd11c*) promoters, respectively. One limitation is that, although CD11c is commonly used as a mouse dendritic cell marker, CD11c is also a cell surface molecule expressed by other immune cells, including lymphocytes and natural killer cells.[25] As such, using CD11c as a promoter for Cre could also generate TLR4 depletion in other immune cells. Furthermore, although *lyz* is highly expressed in all myeloid cells, depletion of TLR4 in this model might also occur in a small population of CD11c^{+} dendritic cells.

In a preliminary study, we further examined the infiltration of osteoclasts and macrophages and expression of *rankl* and *tlr2* among wild-type, TLR4$^{-/-}$, and Lyz-TLR4$^{-/-}$ mice during early skull fracture healing. [**See Figure, Supplemental Digital**

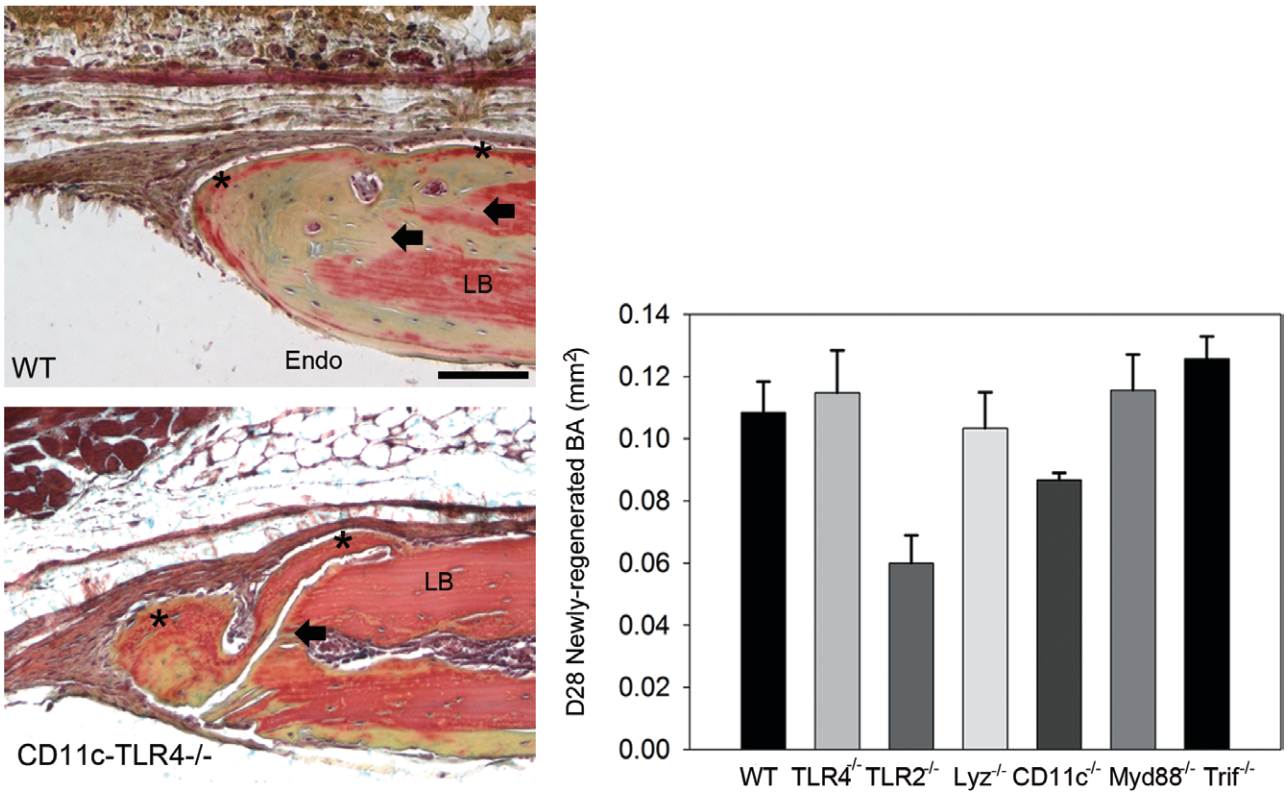

Fig. 4. Histology and histomorphometric analyses of calvarial bone repair at postoperative day 28. (*Left*) Representative pentachrome-stained images of wild-type and CD11c-TLR4$^{-/-}$ mice at day 28. Similar healing was observed among all knockout groups at day 28; thus, CD11c-TLR4$^{-/-}$ mice were used to represent the rest of the knockout mice. Periosteum and soft connective tissue became thinner, denser, and better organized compared with postoperative day 7. Regenerated bone was seen along the dural surfaces of the calvarial bone and along the defect perimeter. Lamellar bone (*asterisk*), which stains positive for acid fuchsin (*red*), was observed in both groups on day 28, suggesting maturation and remodeling of the newly formed bone matrix. (*Below*, *right*) Histomorphometric analysis revealed comparable newly regenerated bone area (*BA*) among all groups on day 28. *Scale bar* = 50 μm. *Arrows*, defect margin; *Endo*, endocortical side; *LB*, lamellar bone.

Content 1, which shows (*left*) representative tartrate-resistant acid phosphatase (TRAP)–stained images at day 7. Tartrate-resistant acid phosphatase–positive osteoclasts were evident at the defect margin and the bone marrow space. At day 7, more intense tartrate-resistant acid phosphatase–positive staining was shown in Lyz-TLR4$^{-/-}$ mice compared with wild-type mice. (*Center*) Representative anti-F4/80–stained images at day 1. Similar anti-F4/80 staining, suggesting comparable macrophage infiltration, was observed in wild-type, TLR4$^{-/-}$, and Lyz-TLR4$^{-/-}$ mice at day 1. (*Above, right*) Similar expression pattern of rankl was shown between TLR4$^{-/-}$ and Lyz-TLR4$^{-/-}$ mice, whereas fold change in expression of these two genes remained relatively unchanged in wild-type mice after surgery. (*Center, right*) Fold change in expression of TLR2 from wild-type, TLR4$^{-/-}$, and Lyz-TLR4$^{-/-}$ mice at 3 hours and days 1 and 4. Significantly higher expression of TLR2 was observed in TLR4$^{-/-}$ mice compared with wild-type and Lyz-TLR4$^{-/-}$ mice at days 1 and 4. Scale bars = 50 μm (n = 3 to 5 per group per time point for histologic analyses, n = 3 to 8 per group per time point for polymerase chain reaction analyses). Mean ± SEM; bold arrow, defect margin; Endo, endocortical side; *p < 0.05 compared to wild-type mice; #compared to Lyz-TLR4$^{-/-}$ mice, ***http://links.lww.com/PRS/C104***.] The results showed more intense staining for the osteoclast marker tartrate-resistant acid phosphatase in Lyz-TLR4$^{-/-}$ mice compared to wild-type mice on day 7, whereas there was no difference in staining for the macrophage marker F4/80 among wild-type, TLR4$^{-/-}$, and Lyz-TLR4$^{-/-}$ mice on day 1. Significantly higher *rankl* expression was found in TLR4$^{-/-}$ compared to wild-type mice on day 4, and significantly higher *tlr2* expression was found in TLR4$^{-/-}$ compared to wild-type and Lyz-TLR4$^{-/-}$ mice on days 1 and 4. These data suggest that loss of TLR4 signaling may lead to enhanced osteoclastogenesis, resulting in faster bone healing response. However, further studies are required to provide more in-depth characterization of both cellular infiltration and the

downstream signaling pathways to elucidate and confirm the underlying mechanisms for rapid bone regeneration.

CONCLUSIONS

We have demonstrated that Toll-like receptor signaling components affect calvarial bone healing, establishing a link between the skeletal and immune systems during craniofacial bone healing. The differential healing responses we observed in knockout mouse models suggest that the $CD11c^{+}$ cells expressing TLR4-mediated MyD88 signaling pathway might be detrimental for calvarial defect healing. However, further work is required to explore the changes in gene expression and cellular infiltration over time during the healing process to improve our understanding of the role of Toll-like receptor–mediated inflammation in bone regeneration. Such data would influence therapeutic design to improve craniofacial bone repair.

Gregory M. Cooper, Ph.D.
B3F3, 3533 Rangos Research Building
530 45th Street
Pittsburgh, Pa. 15201
greg.cooper@chp.edu

ACKNOWLEDGMENTS

The work is supported by the National Science Foundation for Young Scientists of China (no. 81201410) (D.W., principal investigator). The authors are especially grateful to Adam Kubala for assistance in animal surgery, Thomas Prindle (Johns Hopkins University) for assistance in knockout animal cloning and breeding, and Dai Fei Elmer Ker (Stanford University) and Michael Bykowski (University of Pittsburgh) for assistance with editing.

REFERENCES

1. American Association of Neurological Surgeons. *National Neurosurgical Procedural Statistics 2006.* Rolling Meadows, Ill: American Association of Neurological Surgeons; 2006.
2. Mountziaris PM, Spicer PP, Kasper FK, Mikos AG. Harnessing and modulating inflammation in strategies for bone regeneration. *Tissue Eng Part B Rev.* 2011;17:393–402.
3. Mountziaris PM, Mikos AG. Modulation of the inflammatory response for enhanced bone tissue regeneration. *Tissue Eng Part B Rev.* 2008;14:179–186.
4. Balogh ZJ, Reumann MK, Gruen RL, et al. Advances and future directions for management of trauma patients with musculoskeletal injuries. *Lancet* 2012;380:1109–1119.
5. Kaczorowski DJ, Tsung A, Billiar TR. Innate immune mechanisms in ischemia/reperfusion. *Front Biosci (Elite Ed.)* 2009;1:91–98.
6. Rakoff-Nahoum S, Medzhitov R. Toll-like receptors and cancer. *Nat Rev Cancer* 2009;9:57–63.
7. Gao Y, Fang X, Sun H, et al. Toll-like receptor 4-mediated myeloid differentiation factor 88-dependent signaling pathway is activated by cerebral ischemia-reperfusion in hippocampal CA1 region in mice. *Biol Pharm Bull.* 2009;32:1665–1671.
8. Yang QW, Lu FL, Zhou Y, et al. HMBG1 mediates ischemia-reperfusion injury by TRIF-adaptor independent Toll-like receptor 4 signaling. *J Cereb Blood Flow Metab.* 2011;31:593–605.
9. Sachdev U, Cui X, McEnaney R, Wang T, Benabou K, Tzeng E. TLR2 and TLR4 mediate differential responses to limb ischemia through MyD88-dependent and independent pathways. *PLoS One* 2012;7:e50654.
10. Vartanian KB, Stevens SL, Marsh BJ, Williams-Karnesky R, Lessov NS, Stenzel-Poore MP. LPS preconditioning redirects TLR signaling following stroke: TRIF-IRF3 plays a seminal role in mediating tolerance to ischemic injury. *J Neuroinflammation* 2011;8:140–151.
11. Watanabe T, Kobata A, Tanigawa T, et al. Activation of the MyD88 signaling pathway inhibits ischemia-reperfusion injury in the small intestine. *Am J Physiol Gastrointest Liver Physiol.* 2012;303:G324–G334.
12. Wang D, Gilbert JR, Shaw MA, et al. Toll-like receptor 4 mediates the regenerative effects of bone grafts for calvarial bone repair. *Tissue Eng Part A* 2015;21:1299–1308.
13. Xing Q, de Vos P, Faas MM, Ye Q, Ren Y. LPS promotes pre-osteoclast activity by up-regulating CXCR4 via TLR-4. *J Dent Res.* 2011;90:157–162.
14. Kolar P, Schmidt-Bleek K, Schell H, et al. The early fracture hematoma and its potential role in fracture healing. *Tissue Eng Part B Rev.* 2010;16:427–434.
15. Park JE, Barbul A. Understanding the role of immune regulation in wound healing. *Am J Surg.* 2004;187:11S–16S.
16. Geissmann F, Manz MG, Jung S, Sieweke MH, Merad M, Ley K. Development of monocytes, macrophages, and dendritic cells. *Science* 2010;327:656–661.
17. Nace GW, Huang H, Klune JR, et al. Cellular-specific role of toll-like receptor 4 in hepatic ischemia-reperfusion injury in mice. *Hepatology* 2013;58:374–387.
18. Wang D, Gilbert JR, Cray JJ Jr, et al. Accelerated calvarial healing in mice lacking Toll-like receptor 4. *PLoS One* 2012;7:e46945.
19. Eming SA, Hammerschmidt M, Krieg T, Roers A. Interrelation of immunity and tissue repair or regeneration. *Semin Cell Dev Biol.* 2009;20:517–527.
20. Liu Y, Yin H, Zhao M, Lu Q. TLR2 and TLR4 in autoimmune diseases: A comprehensive review. *Clin Rev Allergy Immunol.* 2014;47:136–147.
21. Madeira MF, Queiroz-Junior CM, Cisalpino D, et al. MyD88 is essential for alveolar bone loss induced by *Aggregatibacter actinomycetemcomitans* lipopolysaccharide in mice. *Mol Oral Microbiol.* 2013;28:415–424.
22. Castoldi A, Braga TT, Correa-Costa M, et al. TLR2, TLR4 and the MYD88 signaling pathway are crucial for neutrophil migration in acute kidney injury induced by sepsis. *PLoS One* 2012;7:e37584.
23. Sachdev U, Cui X, Xu J, et al. MyD88 and TRIF mediate divergent inflammatory and regenerative responses to skeletal muscle ischemia. *Physiol Rep.* 2014;2:e12006.
24. Negishi H, Fujita Y, Yanai H, et al. Evidence for licensing of IFN-gamma-induced IFN regulatory factor 1 transcription factor by MyD88 in Toll-like receptor-dependent gene induction program. *Proc Natl Acad Sci USA* 2006;103:15136–15141.
25. Singh-Jasuja H, Thiolat A, Ribon M, et al. The mouse dendritic cell marker CD11c is down-regulated upon cell activation through Toll-like receptor triggering. *Immunobiology* 2013;218:28–39.